Analytical Methods

Accepted Manuscript

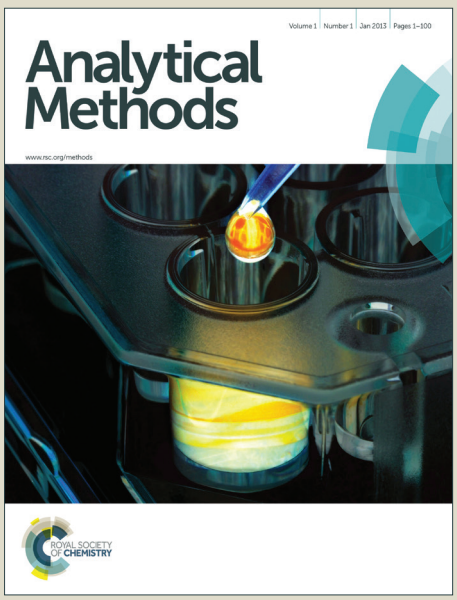

ROYAL SOCIETY OF CHEMISTRY

www.rsc.org/methods

Cite this: DOI: 10.1039/c0xx00000x

www.rsc.org/xxxxxx

ARTICLE TYPE

Chiral glutamic acid functionalized graphene: Preparation and application

Qian Han,[a,b] Qiao Xia[a], Dongmei Guo[a], Can Li[b], Yingzi Fu[a*]

Received (in XXX, XXX) Xth XXXXXXXXX 200X, Accepted Xth XXXXXXXXX 200X

DOI: 10.1039/b000000x

Through the amide group of glutamic acid enantiomer and oxygen-containing groups in graphene oxide, chiral functionalized graphene nanosheets were synthesized, which showed good enantioselective recognition of 3,4-dihydroxyphenylalanine enantiomers. The chiral graphene hybrids should be used as novel promising materials for biological and pharmacological applications.

Chirality comes into our life early, and chiral phenomena have attracted great attention. While still early in its evolution and application, chiral materials are at the point of moving from understanding chirality in the nanoscale, such as functional self-assembly,[1] enantioselective catalysis[2] and optical devices.[3] There has been considerable interest in introducing chirality into solid inorganic materials by organic moieties that could impart some functionality to the solids, for example the adsorption of cysteine enantiomers creates a local chiral envionment on the gold nanoparticles.[4] The synthesis of such chiral inorganic-organic composite materials has been widely reported due to their unique properties and promising potential for a wide range of applications.[5-7]

Graphene, emerging as the monolayer of honeycomb lattice packed with carbon atoms, has received significant attention due to its unique physicochemical properties (high surface area, excellent conductivity, high mechanical strength, and ease of functionalization and mass production).[8] Recently, much effort has been made to prepare functionalized graphene nanocomposites by incorporating organic moieties onto oxygen-containing groups (e.g., hydroxyl, carboxyl, and epoxy) of graphene oxide.[9,10] The amide-functionalized polyhedral oligomeric silsesquioxane was covalently grafted on graphene sheets to increase its solubility in various organic solvents.[11] Poly-L-lysine functionalized graphene was conjugated with horseradish peroxidase to construct a biosensor.[12] However, compared to previous researches, the chiral functionlization of graphene have never been applied to the electrochemical recognition of enantiomers. So the advantages of graphene were perfectly presented in the novel chiral materials for enantioselective recognition.

In this study, we have covalently grafted L-glutamic acid (L-Glu) and D-glutamic acid (D-Glu) onto graphene sheets via the amide formation between amino groups of glutamic acid enantiomers and oxygen-containing groups (e.g., epoxy and carboxyl groups) in graphene oxide. The resultant L-glutamic acid graphene hybrid (LGO) and D-glutamic acid graphene hybrid (DGO) are found to be of high chiral property and excellent electrochemical activity towards electroactive 3,4-dihydroxyphenylalanine (DOPA) enantiomers.

For the preparation of the LGO or DGO hybrids, the 7 mg of graphene oxides were mixed with 28 mg of L-Glu or D-Glu, and 35 mg KOH in 35 ml H_2O at 70 °C for 24 h, and then the mixture was reduced with 3.5 ml $NaBH_4$ (0.2 mol L^{-1}) solution at 70 °C for 2 h. After reduction, a black dispersion was obtained, and the excess of impurities was removed with five successive cycles that involved centrifugation, decantation, and exsiccation to ultimately yield LGO or DGO hybrids.

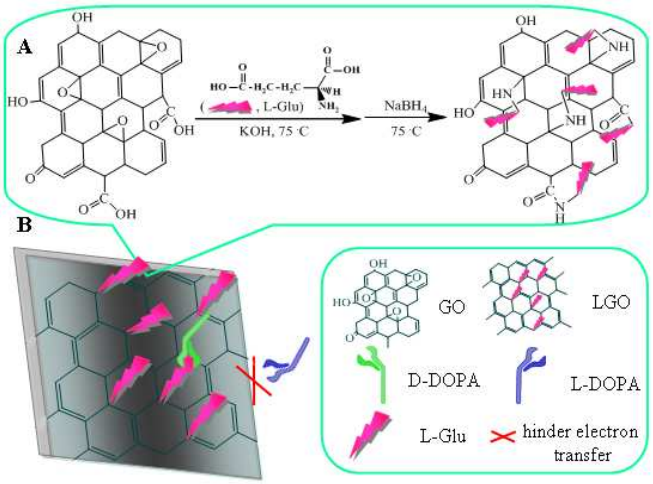

Scheme 1 (A) Schematic representation of the synthesis of multifunctional LGO nanohybrids. (B) The mechanism of the chiral recognition strategy

As shown in Scheme 1A, take the case of L-Glu, the LGO was covalently grafted to graphene through the reaction of epoxy groups on graphene oxides and amino groups on L-Glu in the presence of KOH.[13] Fourier transform infrared spectroscopy (FTIR) was used to obtain the structural information (Fig. 1A). The spectrum of graphene oxide shows the presence of hydroxyl (3444 cm^{-1}), unsaturated C-H bands (3156 cm^{-1}), carbonyl (1632 cm^{-1}) and epoxy (910 cm^{-1}) groups.[14] The FT-IR spectrum of L-Glu and D-Glu exhibited free amino groups at 3400~3500 cm^{-1}, the symmetric stretch of C-N at 1352 cm^{-1}, and the carbonyl at

about 1600~1700 cm^{-1}. After chemical attachment of Glu enantiomers onto the graphene oxide, the characteristic bands of oxide groups (νO-H, νC=O and νC-O) shifted greatly, the FTIR spectrum of LGO and DGO exhibited absorption features of Glu enantiomers. Especially, the peak of the amide C-N stretch mode in LGO and DGO appeared at 1352 cm^{-1}. The disappearance of epoxy (910 cm^{-1}) groups in LGO and DGO indicated that graphene oxides such have been fully reduced to chiral graphene nanocomposite. These results confirmed that L-Glu and D-Glu have been chemically grafted onto grapheme. The reduction of graphene oxides was also indicated from the color change of solution before and after reaction (from brown to dark, see the supplementary information Fig.S1). At concentrations of 0.5 $mg \cdot mL^{-1}$, the resulting LGO and DGO aqueous solution was very stable without precipitation even after 24 h storage, which is very favorable for the further applications of this functionalized graphene.

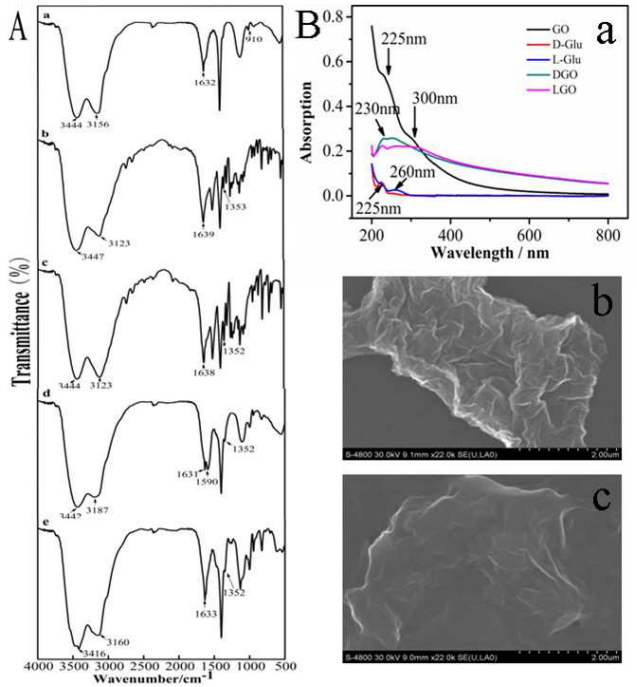

Fig.1 (A) FTIR spectra of (a) graphene oxides, (b) L-glutamic acid, (c) D-glutamic acid, (d) L-glutamic acid-graphene hybrid and (d) D-glutamic acid-graphene hybrids. (B) (a) UV-vis spectra of GO, D-Glu, L-Glu, and LGO, DGO hybrids. SEM images of (b) LGO and (c) DGO.

In order to confirm the formation of the LGO and DGO hybrids, the UV–vis absorption spectra of GO, L-Glu, D-Glu, LGO and DGO were recorded, as shown in Fig.1B a. The UV–vis spectra of GO showed a strong absorption band at 225 nm and 300 nm, attributing to the π-π* transition of aromatic C-C bonds. The Glu spectrum exhibited an absorption at 225 nm and 260 nm, while the absorbance of the hybrids exhibits a broad absorption in the range from 230 nm to 280 nm, and compared with GO, the absorption in the all scanned wavelength was wide and decreased. It was noted that the L-Glu and D-Glu nanocomposites were covalently grafted to the graphene. The ratio of GO/L-Glu, pH and the temperature all affect the praparation of hybrids. UV-Vis absorption spectroscopy was used to monitor the effect of these factors on the reduction process (supplementary information Fig.S2). Take the LGO as an example, the amount of L-Glu was investigated (Fig. S2a, pH=13.0). When the GO/L-Glu ratio was decreased continually, λmax shifted to a higher wavelength and reached 280nm. When the GO/L-Glu ratio (w/w) was lower than 1:4, λmax shifted little. Considering a sufficient reaction, the ratio of L-Glu to GO was 1:4. The pH value has a significant influence on the synthetic materials (Fig.S2b). The alkaline conditions were favorable for ring-opening reaction of epoxide and amine hydrogen. The pH effect of the solution was studied from pH 8.0 to 14.0. It showed that the absorption peak shifted to 280nm at pH 13.0 and the increasing pH value could not cause a further change in λmax. Hence, the solution pH of 13.0 was selected in the synthesis experiment. The effect of the temperature on the chiral hybird was also investigated (Fig.S2c). When the GO reduction was carried out at 50°C and 60°C, the λmax only shifted to 245, 261nm, respectively. When the reaction temperature was increased from 65°C to 80°C, the λmax shifted to 280 nm, and the further increasing temperature could not cause obvious shift. Thus, 70°C was chosen as the optimal reaction temperature.

The morphology and microstructure of as-prepared chiral materials were investigated by scanning electron microscopy (SEM), SEM image showed the almost thin gossamer shapes of LGO and DGO hybrids (Fig.1B b and c). The mean dimension of the LGO and DGO was found to be nano-size, it presented nanosized chiral spaces as the enantioselective site.

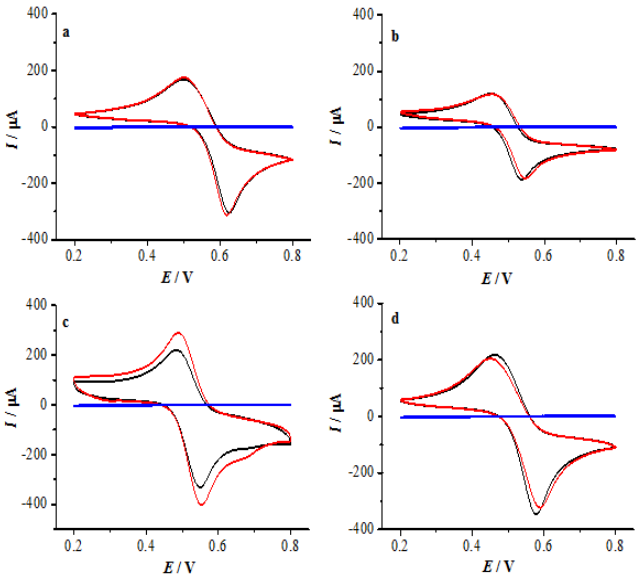

Fig.2 Cyclic voltammograms for L-DOPA (black) and D-DOPA (red) and 0.25 M H_2SO_4 solution in absence of DOPA (blue) on (a) bare GCE, (b) GO/GCE, (c) LGO/GCE, and (d) DGO/GCE, respectively. The concentration of DOPA was 5 mM in 0.25 M H_2SO_4. The scan rate was 100 $mV \cdot s^{-1}$.

To apply the chiral materials in a potential field, an attempt was made to construct a chemically modified electrode for chiral recognition. Fig.2 shows cyclic voltammetrys (CV) for DOPA on different modified electrodes. As shown in Fig.2a, DOPA displayed well-defined redox waves on bare glassy carbon electrodes (GCE). The redox peaks appeared around 0.5001 V and 0.6190 V at scan rate of 100 mV s^{-1} due to two-electron–two-proton oxidation and reduction of the DOPA/dopaquinone couple.[16] The electrochemical behavior of DOPA on graphene oxide modified electrodes (denoted as GO/GCE) was similar to that on bare GCE, and small current values for DOPA enantiomers were observed (Fig.2b). The interference of the 0.25

M H_2SO_4 on different electrodes has been investigated (Fig. 2 blue line). The peak current of DOPA is much larger than the background current, so background interference maybe negligible. After LGO was immobilized on GCE (LGO/GCE), the surface pKa_1 and pKa_2 were estimated to be 6.00 ± 0.01 and 8.00 ± 0.01 from the peak of the differential curve of the experiment data (supplementary information Fig.S4)[17], small ΔE values were showed for L- or D-DOPA on the LGO modified electrodes (Fig.2c), the redox currents of DOPA enantiomers on LGO/GCE were much larger than that on bare GCE. The oxidation and reduction peak currents of D-DOPA were 288.7 μA and -402.9 μA, while a relative narrow voltammograms was observed for L- DOPA and the values of peak current were 220.2 μA and -330.0 μA, respectively. For the DGO modified electrode (DGO/GCE), the values of oxidation and reduction peak currents of L-DOPA and D-DOPA were all different, even the redox currents of L-DOPA were much larger than that of D-DOPA (Fig.2d). The results exhibited that the electron transfer of L- and D-DOPA on LGO/GCE was favored and LGO modified electrode presented stronger electrocatalytic ability to D-DOPA than L-DOPA. The voltammetric datas of DOPA were analyzed more deeply (supplementary information Fig. S5), the redox peak current increased with the scan rates in the range from 50 to 200 mV s^{-1}, the peak current density and the square root of potential scan rate presented a linear relationship. It corroborated that the electron transfer reaction was controlled by the diffusion of DOPA.

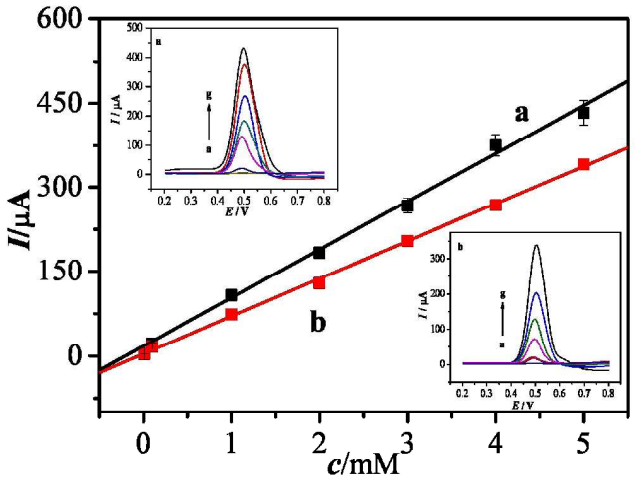

Fig.3 The linear response of the chiral LGO/GCE electrode with different concentrations of (a) D-DOPA, (b) L-DOPA (from a to g): 0.005, 0.1, 1.0, 2.0, 30, 4.0 and 5.0 mM. The inset shows the DNPV responses of different concentrations of a) D-DOPA, (b) L-DOPA.

Table 1 The comparison of analytical performances of different electrochemical sensors for L-DOPA and D-DOPA determination.

Electrode	DOPA isomer	linear range (mM)	detection limit (mM)	ΔI^b (μA)	Reference
SWCNTs/GCE	L-DOPA	2.5×10^{-3}～0.2mM	NR	20	20
	D-DOPA	2.5×10^{-3}～0.2 mM	NR		
L -NIBC-Au	L-DOPA	NR	NR	33.62	21
	D-DOPA	NR	NR		
PLL/GCE	L-DOPA	1.0×10^{-3} ～8.0 mM	3.3×10^{-4}mM	42.33	19
	D-DOPA	5.0×10^{-4} ～8.0 mM	1.7×10^{-4}mM		
LGO/GCE	L-DOPA	5.0×10^{-3} ～5.0 mM	2.3×10^{-4}mM	72.9	this work
	D-DOPA	5.0×10^{-3}～5.0 mM	1.7×10^{-4}mM		

[a] Footnote. NR, not reported; SWCNTs, single-walled carbon nanotubes; NIBC, N-isobutyryl-l-cysteine ; PLL/GCE, poly-l-lysine matrix (PLL) modified GCE; LGO, L-glutamic acid graphene hybrid;

DNPV techniques were employed to investigate the voltammetric behaviors of DOPA enantiomers because of its higher sensitivity compared to CV. Fig. 3a showed the calibration curves of the anodic peak current values of L-DOPA on the modified electrode in the linear range from 5.0×10^{-3} mM to 5.0 mM with the regression equation of $Ip(\mu A) = 66.35c$ (mM) + 4.814 and D-DOPA with the regression equation $Ip(\mu A) = 86.56c$ (mM) + 12.08 (Fig.3b). The correlation coefficients of 0.9984, and 0.9955, respectively. The detection limit (DL) of L-DOPA and D-DOPA were 2.261×10^{-4} mM and 1.733×10^{-4} mM, respectively, in terms of the role of signal to noise ratio of 3:1 (S/N=3). From the differences in peak potential of DNPV, the relative energetic differences (ΔG) for the electron transfer of L-DOPA and D-DOPA on LGO surface can be derived[18,19]. The Gibbs' energy of L-DOPA (or D-DOPA) enantiomer were -4.593 KJ·mol^{-1} and -6.252 KJ·mol^{-1} at 25°C.

The DNPV was used to investigate the presence of AA on the behavior of 2mM D-DOPA (supplementary information Fig.S7). The AA signal was visible at about 1.41V, the presence of 5-fold excess of AA did not interfere the response of DOPA at 0.552V. Table 1 showed the comparison for the determination of DOPA enantiomers at LGO/GCE electrode with various modified electrodes based on literature reports. It showed that the proposed method in this work was perferable in enantioselective recognition of DOPA enantiomers.

In addition, the resultant functionalized graphene facilitate the redox reaction of only one enantiomer of 3,4-dihydroxyphenylalanine, and the chiral recognition was more inclined to the heterochiral interaction between LGO (DGO) and D- (L-) DOPA, the oxidation peak intensity of DOPA in heterochiral interactions was larger than that in homochiral interactions (Scheme 1B). Take the L-glutamic acid graphene hybrid, for example, it was suggested to block the redox reaction of L-DOPA, but tended to cross inversion for the incongruous enantiomer D-DOPA. These results were similar to the enantioselective redox reaction of DOPA at chiral molecule

modified electrodes. [2, 22] To gain a deep explanation of a highly selectivity for DOPA enantiomers, achiral GO was used to detect DOPA enantiomers in Fig.2b, L- and D-DOPA display almost the same electrochemical response. This suggests that the enantiomers could not be discriminated without a chiral environment, and thus the chiral construction is critically important for chiral recognition.

In summary, novel functionalized graphene nanocomposites were synthesized by covalent modification with Glu enantiomers, respectively. The graphene nanocomposite as a chiral sensor platform not only presented suitable chiral spaces as the enantioselective site for targets but also played a role of fast electron-transfer kinetics and further signal amplification in electrochemical detection of DOPA enantiomers. Therefore, the chiral materials of graphene represent a huge step toward technological applications of graphene, even toward chiral discrimination in pharmacology and biomedicine.

The authors are grateful for the financial supports provided by the National Natural Science Foundation of China (21272188). Natural Science Foundation for Young Scientists of Hebei Province, China (B2015205169).

Notes and references

[a]*Key Laboratory on Luminescence and Real-Time Analysis, Ministry of Education, College of Chemistry and Chemical Engineering, Southwest University, Chongqing 400715, PR China. Corresponding author: Fax: +86-023-68253195; Tel: +86-023-68252360; E-mail address: fyzc@swu.edu.cn*

[b]*Laboratory of Environment change and Ecological Construction of Hebei Province, College of Resources and Environment Science, Hebei Normal University, Shijiazhuang, Hebei 050024, PR China.*

† Electronic Supplementary Information (ESI) available: [details of any supplementary information available should be included here]. See DOI: 10.1039/b000000x/

1 J.J. Ryoo, J.W. Shin, H.S. Dho,and K.S. Min, *Inorg. Chem.*, 2010, **49**, 7232.

2 Y.J. Kang, J.W. Oh, Y.R. Kim, J.S. Kim and H. Kim, *Chem. Commun.*, 2010, **46**, 5665.

3 P. Paik, A.Gedanken and Y. Mastai, *J. Mater. Chem.*, 2010, **20**, 4085.

4 I. S. Lim, D. Mott, M.H. Engelhard, Y. Pan, S.Kamodia, J. Luo, P.N. Njoki, S.Q. Zhou, L.C. Wang, and C.J. Zhong, *Anal. Chem.*, 2009, **81**, 689.

5 V. Kitaev, *J. Mater. Chem.*, 2008, **18**, 4745.

6 M.O. Lorenzo,C.J. Baddeley, C. Muryn, R. Raval, *Nature*, 2000,**404**, 376-379

7 Y.Z. Fu, M. Chen, X. Cui, L.L. Wang, Q. Chen, J. Zhou, *Sci China Chem.,* 2010, **53***,* 1453.

8 D. Chen, L.H. Tang and J.H. Li, *Chem.Soc.Rev.*, 2010, **39**, 3157.

9 C.H. Jin, J. Lee, E. Lee, E. Hwang and H. Lee, *Chem. Commun*., 2012, **48**, 4235.

10 W.L.Wei, K.G. Qu, J.S. Ren and X.G. Qu, *Chem. Sci.*, 2011, **2**, 2050.

11 Y.H. Xue, Y. Liu, F. Lu, J. Qu, H. Chen, and L.M. Dai, *J. Phys. Chem. Lett.* 2012, **3**, 1607.

12 C.S. Shan, H.F. Yang, D.X. Han, Q.X. Zhang, A.Ivaska, and L. Niu, *Langmuir*, 2009, **25** (20) 12030.

13 T. Szabo, O. Berkesi, P. Forgo, K. Josepovits, Y. Sanakis, D. Petridis, I. Dekany, *Chem. Mater.*, 2006, **18**, 2740.

14 K. Mao, D. Wu, Y. Li, H. Ma, Z. Ni, H. Yu, C. Luo, Q. Wei, B. Du, *Anal. Biochem.*, 2012, **422**, 22.

15 Y. Imai, K. Murata, Y. Nakano, T. Harada, T. Kinuta, N. Tajima, T. Sato, M. Fujiki, R. Kurodace and Y. Matsubara, *CrystEng Com*m, 2010, **12**, 1688.

16 X.Q. Liu, Z.L. Zhang, G.J. Cheng, S.J. Dong, *Electroanalysis*, 2003, **15**, 103.

17 J.W. Zhao, L.Q. Luo, X.R. Yang, E. Wang, S.J. Dong. Electranalysis. 1999, **11**(15), 1108.

18 X.Q. Liu, Z.Zhang, G.J. Cheng and S.J. Dong, *Electroanalysis.* 2003, **15**, 107.

19 Y.H. Huang, Q. Han, Q. Zhang, L. Guo, D. Guo, Y.Z. Fu. Electrochim. Acta, 2013, **113**, 564.

20 L.S. Chen, F.X. Chang, L.C. Meng, M.X. Li and Z.W.Zhu, Analys t ,2014, **139**, 2243.

21 Q. Han, Q. Chen, Y.H.Wang, J. Zhou , Y. Fu, Electroanalysis, 2012, **24**(2), 332.

22 T. Nakanishi, M. Matsunaga, M. Nagasaka, T. Asahi, and T. Osaka, *J. Am. Chem. Soc.* 2006, **128**, 13322.